Journal of Colloid and Interface Science 423 (2014) 25–32

Contents lists available at ScienceDirect

Journal of Colloid and Interface Science

www.elsevier.com/locate/jcis

Fe(III) oxides accelerate microbial nitrate reduction and electricity generation by *Klebsiella pneumoniae* L17

Tongxu Liu [1], Xiaomin Li [1], Wei Zhang, Min Hu, Fangbai Li *

Guangdong Institute of Eco-Environmental and Soil Sciences, Guangzhou 510650, PR China

ARTICLE INFO

Article history:
Received 18 October 2013
Accepted 21 February 2014
Available online 28 February 2014

Keywords:
Iron oxide
Nitrate reduction
Electricity generation
Klebsiella pneumoniae L17

ABSTRACT

Klebsiella pneumoniae L17 is a fermentative bacterium that can reduce iron oxide and generate electricity under anoxic conditions, as previously reported. This study reveals that *K. pneumoniae* L17 is also capable of dissimilatory nitrate reduction, producing NO_2^-, NH_4^+, NO and N_2O under anoxic conditions. The presence of Fe(III) oxides (i.e., α-FeOOH, γ-FeOOH, α-Fe_2O_3 and γ-Fe_2O_3) significantly accelerates the reduction of nitrate and generation of electricity by *K. pneumoniae* L17, which is similar to a previous report regarding another fermentative bacterium, *Bacillus*. No significant nitrate reduction was observed upon treatment with Fe^{2+} or α-FeOOH+Fe^{2+}, but a slight facilitation of nitrate reduction and electricity generation was observed upon treatment with L17+Fe^{2+}. This result suggests that aqueous Fe(II) or mineral-adsorbed Fe(II) cannot reduce nitrate abiotically but that L17 can catalyze the reduction of nitrate and generation of electricity in the presence of Fe(II) (which might exist as cell surface-bound Fe(II)). To rule out the potential effect of Fe(II) produced by L17 during microbial iron reduction, treatments with the addition of TiO_2 or Al_2O_3 instead of Fe(III) oxides also exhibited accelerated microbial nitrate reduction and electricity generation, indicating that cell-mineral sorption did account for the acceleration effect. However, the acceleration caused by Fe(III) oxides is only partially attributed to the cell surface-bound Fe(II) and cell-mineral sorption but may be driven by the iron oxide conduction band-mediated electron transfer from L17 to nitrate or an electrode, as proposed previously. The current study extends the diversity of bacteria of which nitrate reduction and electricity generation can be facilitated by the presence of iron oxides and confirms the positive role of Fe(III) oxides on microbial nitrate reduction and electricity generation by particular fermentative bacteria in anoxic environments.

1. Introduction

Extracellular electron transfer refers to the use of a substrate as a terminal electron acceptor that interacts with a protein in the cellular electron transport chain, which resides on the cell surface [1,2]. The use of such substrates has been extensively explored through studies concerning the reduction of dissolved substrates (e.g., nitrate, sulfate, and humic substances), poorly soluble substrates (e.g., iron and manganese minerals) and insoluble substrates (e.g., electrodes) [3,4]. This not only influences the biogeochemical cycling of organic and inorganic elements [3–6], but has also been applied for electricity generation in microbial fuel cells (MFCs) [7–9]. A number of microorganisms, such as *Shewanella*, *Geobacter*, *Dechloromonas*, and *Desulfotomaculum* species, have been reported to oxidize organic electron donors coupled with the reduction of many electron acceptors [3,10–12]. When such electron acceptors coexist in the natural environment, complicated interactions with one another (e.g., inhibition and enhancement) have been observed. Fe(III) has been reported as a strictly competitive electron acceptor with respect to the reduction of other substrates by these organisms [3–5,13]. However, whether Fe(III) oxides can influence extracellular electron transfer in other organisms remains unknown.

Klebsiella pneumoniae L17 is a fermentative bacterium that has been reported to be capable of reducing minor amounts of Fe(III) during glucose fermentation [14] and using an electrode as electron acceptor for the generation of electricity under anoxic conditions [15]. Dissimilatory iron(III)-reducing bacteria (DIRB), which use iron(III) as a terminal electron acceptor in respiration, are responsible for most of the iron(III) reduction in soils and sediments [3,16]. Fermentative microorganisms in iron-reducing environments are considered to be responsible for the production of fermentation products that serve as electron donors for DIRB. Although many fermentative microorganisms demonstrate a weak ability for Fe(III) reduction, their abundance is one or two orders of magnitude higher than DIRB [17]. Previous investigations regarding the effect of iron oxide on the reduction of other electron

* Corresponding author. Fax: +86 20 87024123.
E-mail address: cefbli@soil.gd.cn (F. Li).
[1] Tongxu Liu and Xiaomin Li contributed equally to this work.

http://dx.doi.org/10.1016/j.jcis.2014.02.026
0021-9797/

acceptors by microorganisms have mainly focused on DIRB, such as *Shewanella* and *Geobacter*, with results indicating that the presence of iron oxide inhibits microbial nitrate reduction [18–23]. The effect of Fe(III) oxides on the reduction of other coexisting substrates may also be influenced by fermentative microorganisms.

Among the reduction processes of soluble substrates, nitrate reduction plays a key role in the nitrogen cycle and has important agricultural, environmental, and public health implications [24]. It is predominantly attributed to the biotic process of direct enzyme catalysis by nitrate-reducing bacteria [25,26]. Many *Klebsiella* species are able to use nitrate and its reduction product, nitrite, as electron acceptors for anaerobic respiration (dissimilatory nitrate reduction) [27,28], or as nitrogen sources for biosynthesis (assimilatory nitrate reduction) [29,30]. In addition, nitrate can be reduced by dumping excess electrons onto oxidized nitrogen species during microbial fermentation [28]. The ability of *K. pneumoniae* L17 to reduce nitrate remains unclear. Natural nitrate reduction is usually coupled with iron cycles in iron-bearing subsoils or sediments [6,31]. Nitrate reduction can be microbially catalyzed and coupled to the oxidation of dissolved or solid-phase Fe(II) compounds (nitrate-dependent Fe(II) oxidation) in the pure culture of isolates [31,32] and in sediment-enriched culture under anoxic conditions [33,34]. The abiotic reduction of nitrate to ammonium by Fe(II) at pH $\geqslant$ 8.0 occurs in the presence of green rust [35], or Cu^{2+} with or without iron oxides [36]. However, few studies have considered the effect of Fe(III) oxide on nitrate reduction by *Klebsiella* species.

Thus far, the subject of extracellular electron transfer has been explored mostly through studies concerning the reduction of iron and manganese minerals [1]. Recently, anodes in MFCs have been used as important insoluble electron acceptors to investigate extracellular electron transfer in microorganisms [37]. Microorganisms generate current mainly via outer membrane proteins, microbially secreted chelators, electron shuttles, and possibly through nanowires (e.g., electrically conductive pili) [1,2]. The addition of soluble mediators (e.g., humic acid) also accelerates electron transfer from microorganisms to anodes in MFCs [38]. Nakamura et al. [39] reported that iron oxides facilitate long-distance electron transport via constructing electrically conductive networks containing iron nanoparticles and DIRB. *K. pneumoniae* L17 (referred to as L17 from this point forward) has also been reported to be an electroactive bacterium for electricity generation [15]. However, the effect of Fe(III) oxides on electricity generation by L17 has not been investigated.

A previous study reported that the presence of iron oxides can accelerate the nitrate reduction and current generation by a fermentative *Bacillus* sp. [40], which is different from the previously reported inhibitory effect of Fe(III) oxides on nitrate reduction by DIRB [18–23]. However, it remains unclear whether the acceleration effect of iron oxide occurs with microbial nitrate reduction and current generation in other fermentative bacteria. In this study, the nitrate reduction ability of L17 was investigated under anoxic conditions. Compared with the previous study of *Bacillus*, the current study provides more details about the reaction pathway of nitrate reduction by L17 using biochemical and molecular biological analysis and via determination of gaseous phase intermediates. The addition of Fe(III) oxides was also found to accelerate the reduction of nitrate and generation of electricity by L17. The potential roles of different forms of Fe(II) produced by L17 in the reduction of nitrate and generation of electricity are also discussed based on different treatments, including Fe(II), Fe(II) + α-FeOOH and L17 + Fe(II). Non-Fe(III) oxides, i.e., TiO_2 and Al_2O_3, were used in place of Fe(III) oxides to avoid the potential effects of Fe(II) generated by L17 and to evaluate the effect of cell-mineral sorption. Potential mechanisms for the accelerating effect of Fe(III) oxides on nitrate reduction and electricity generation by L17 are discussed based on the obtained results.

2. Materials and methods

2.1. Materials

K. pneumoniae L17 was previously isolated from subterranean forest soil in Zhaoqing, China [14]. Three Fe(III) oxides were synthesized as described previously [14], in which goethite (α-FeOOH) was prepared by dissolving $Fe(NO_3)_3{\cdot}9H_2O$ in potassium hydroxide; lepidocrocite (γ-FeOOH) was synthesized by mixing $FeCl_2{\cdot}4H_2O$, $(CH_2)_6N_4$, and $NaNO_2$ in deionized water; hematite (α-Fe_2O_3) was formed by sintering γ-FeOOH powder at 420 °C for 2 h at a temperature increase rate of 2 °C min^{-1}. Maghemite (γ-Fe_2O_3) was synthesized using $FeCl_2$, $(CH_2)_6N_4$, and $NaNO_3$ [41]. TiO_2 (Degussa P-25, with 80% anatase and 20% rutile) was obtained from Degussa AG Company, Germany. Al_2O_3 (Alu-C, 13 nm) was purchased from Sigma–Aldrich. All of the Fe(III) and non-Fe(III) oxides were ground and passed through a 100-mesh sieve before use. The X-ray diffraction (XRD) patterns of four Fe(III) oxides are shown in Fig. S1. The surface areas measured using the Brunauer–Emmett–Teller (BET) method were 120.93 $m^2 g^{-1}$ (α-FeOOH), 115.44 $m^2 g^{-1}$ (γ-FeOOH), 29.40 $m^2 g^{-1}$ (α-Fe_2O_3), 14.36 $m^2 g^{-1}$ (γ-Fe_2O_3), 50 $m^2 g^{-1}$ (TiO_2), and 220 $m^2 g^{-1}$ (Al_2O_3). $NaNO_3$ ($\geqslant$99.0%), $NaNO_2$ (99.5%), $FeSO_4{\cdot}7H_2O$ ($\geqslant$99.0%), and Nessler's reagent were purchased from Sigma–Aldrich and used without further purification. Other chemicals were of analytical grade and were purchased from Guangzhou Chemical Reagent Factory, China.

2.2. Nitrate reduction

At first, goethite was chosen as the model Fe(III) oxide because it is one of the naturally common Fe(III) oxyhydroxides in soil, especially in subtropical iron-rich red soils. Six batch experiments for NO_3^- or NO_2^- reduction were conducted: (1) Fe(II), (2) α-FeOOH, (3) Fe(II) + α-FeOOH, (4) L17, (5) L17 + Fe(II), and (6) L17 + α-FeOOH. Equivalent weights of other Fe(III) and non-Fe(III) oxides were then used to verify our finding and elucidate a possible mechanism. L17 cells were grown in a nutrient broth (consisting of peptone (10 g L^{-1}), beef extract (3 g L^{-1}), and NaCl (5 g L^{-1}) at pH = 7.0 ± 0.2) under oxic conditions on a rotary shaker at 180 rpm and 30 °C and harvested by centrifugation at 6900*g* for 10 min at 4 °C when the culture approached the exponential phase. The pellets were washed with sterile deionized water three times, after which they were resuspended in sterile deionized water. The initial concentrations of $NaNO_3$ or $NaNO_2$, Fe(II), and α-FeOOH were 7.5 mM, 0.3 mM, and 4.5 g L^{-1}, respectively. The harvested L17 cells had a final concentration of ca. 10^7 cells mL^{-1} and were added into an anoxic $NaHCO_3$-buffered (30 mM, pH 6.8, with N_2:CO_2 = 80:20 atmosphere) medium in the presence of 5.0 mM glucose, which served as the carbon source. Anaerobic techniques were used throughout all experiments, as previously described [14]. Inoculation and sampling were conducted using sterile syringes and needles. All trials (25.2-mL serum bottle with 5.2-mL headspaces, capped with butyl rubber closures, and crimp sealed) were conducted in triplicate and incubated in a BACTRON Anaerobic/Environmental Chamber II (SHELLAB, Sheldon Manufacturing Inc.) at 30 °C in the dark.

2.3. Electricity generation

Microbial electricity generation was tested using a bioelectrochemical (BEC) reactor, as shown in Fig. S2. To operate the BEC reactor, a suspension of harvested L17 cells (ca. 10^7 cells mL^{-1}) and/or Fe(II) (0.3 mM) or oxides (4.5 g L^{-1}) in the $NaHCO_3$-buffered (30 mM, pH 6.8) medium containing glucose (5.0 mM), was added into the anode chamber under a N_2:CO_2 = 80:20 atmosphere.

Abiotic treatments of Fe(II) and Fe(II) + α-FeOOH with the same initial concentrations were conducted in the same buffer without glucose. Catholyte containing 0.2 M potassium ferricyanide was added to the cathode chamber under atmospheric pressure. All experiments were conducted at a controlled temperature of 30 °C. A 1000 Ω resistor was used as an external load. To confirm the repeatability using different reactors, reactions were conducted simultaneously in two reactors containing suspensions of L17. The results indicated that electricity generation in the two reactors had a low standard deviation based on the total coulombs (<10%). The same quantity of other Fe(III) oxides (i.e., γ-FeOOH, α-Fe_2O_3, and γ-Fe_2O_3) was added into the cell suspension in the anodic chamber of the BEC to confirm the acceleration effect of added α-FeOOH.

2.4. Analytical methods

The surface area was measured using the BET method with a Coulter SA-3100, in which N_2 adsorption at 77 K was applied and a Carlo Erba sorptometer was used. The surface complexation model calculation using Visual MINTEQ 3.0 software demonstrated that neither nitrite nor ammonium was adsorbed onto the α-FeOOH surface in the $NaHCO_3$-buffered medium (pH 6.8). Therefore, adsorbed nitrite and ammonium species were ignored. To determine NO_3^-/NO_2^- and NH_4^+, samples were filtered using a syringe filter containing a 0.22-μm mixed cellulose ester membrane after centrifugation at 8500*g* for 20 min to remove cells and oxides and exposed to O_2 to rapidly oxidize Fe(II) [42]. The concentration of NO_3^-/NO_2^- was determined by ion chromatography (Dionex ICS-90) with an ion column (IonPac AS14A 4 × 250 mm). A mobile phase containing Na_2CO_3 (8.0 mM) and $NaHCO_3$ (1.0 mM) was operated at a flow rate of 1.0 mL min^{-1}. The detection limits by the ion chromatography analysis were approximately 0.003 mM for both NO_3^- and NO_2^-. The concentration of NH_4^+ was measured by spectrophotometry at 420 nm after a colorimetric reaction with Nessler's reagent [43]. Before Nessler's reagent was added, an aliquot of the sample to be analyzed was diluted with ultrapure water. Ammonium chloride solutions were used as standards. The concentrations of dissolved and adsorbed Fe(II) were determined as previously described [14]. The analysis of Fe(II) in NO_3^--containing samples was performed using a sequential extraction technique [13]. The nitrite was removed prior to acidifying the sample to extract adsorbed Fe(II) because nitrite rapidly oxidizes Fe(II) in acidic solution. Experimental procedures for measuring nitrate reductase (*nar*Z) and nitrite reductase (*nir*B) gene were described in Supporting Information. The N_2O and NO levels in the liquid and gas phases were measured online by a commercially available profiler (Unisense; Århus, Denmark) equipped with N_2O and NO microelectrodes. Trials for determination of N_2O and NO were conducted in 500-mL bottles with 400-mL headspaces. Confocal laser scanning microscope (CLSM) was employed to test the cell-mineral sorption after 1 d incubation, wherein 1 mL of suspension with cells and α-FeOOH was stained with a Live–Dead dye (L-7012, Molecular Probes, Eugene, OR, USA) for 5 min and then sealed under a 1 mm thick coverslip for examination. Specimens were examined with a Leica TCS-SP2 CLAM (Leica Microsystems Heidelberg GmbH, Germany), which was operated at an illumination length of 488 nm in both fluorescence and reflectance modes.

3. Results and discussion

3.1. Nitrate reduction by K. pneumoniae L17

As shown in Fig. 1a, NO_3^- was completely reduced by L17 in the presence of glucose after 4 d of incubation with a pseudo-first-order reaction rate constant (*k*) of 0.855 d^{-1} (R^2 = 0.974), as shown in the figure inset, which is higher than that of *Bacillus* in reported in a previous study [40]. NO_2^-, which is the first reduced intermediate of NO_3^-, increased over time at the beginning of the incubation, achieved its highest concentration on the 4th day, and then decreased after NO_3^- was completely reduced (Fig. 1b). NH_4^+ was detected as one of the end products of nitrate reduction, which increased significantly from the 4th day (Fig. 1c). Our preliminary results indicated that only 3.58% of the initial nitrate was reduced to nitrite by L17 without glucose after 1 d of incubation, and no

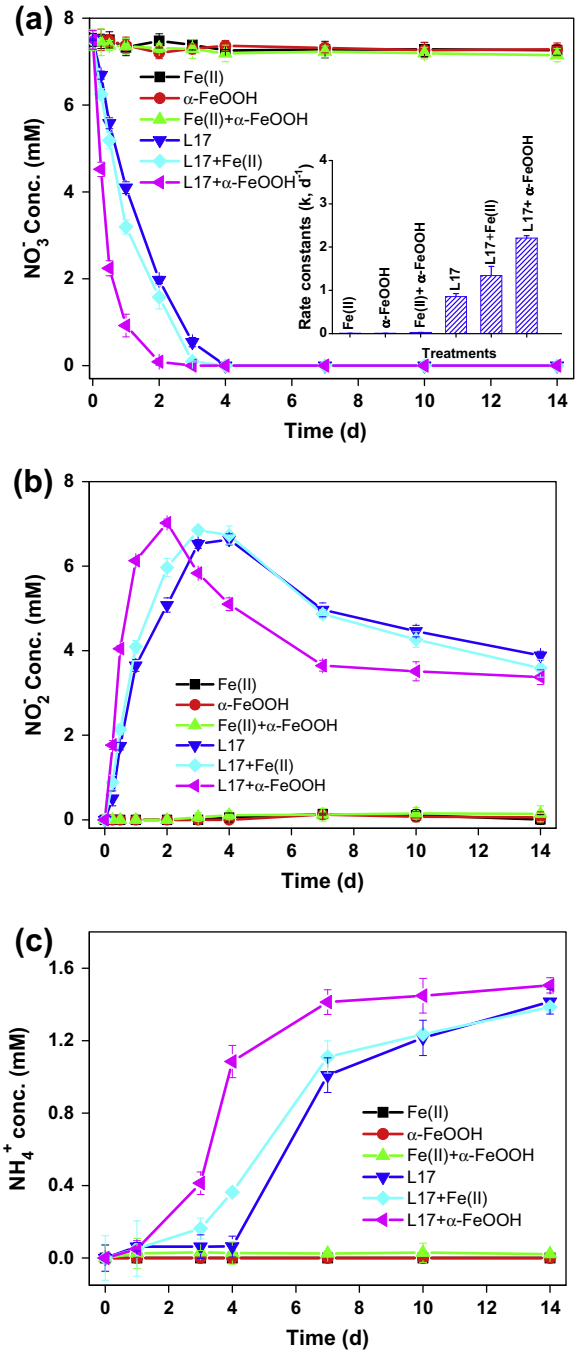

Fig. 1. (a) NO_3^- reduction with the pseudo-first-order rate constants shown in the inset, (b) NO_2^- formation, and (c) NH_4^+ formation under various treatments. Initial concentrations: 7.5 mM NO_3^-, 0.3 mM Fe(II), 4.5 g L^{-1} α-FeOOH, 10^7 L17 cells mL^{-1}, and 5.0 mM glucose in a 30 mM $NaHCO_3$-buffered medium at pH = 6.8. Glucose was added in all biotic treatments with L17. Error bars represent the standard deviation of the mean (*n* = 3).

nitrate reduction was detected with glucose alone or with dead cells + glucose (Fig. S3). The fact that significant nitrate reduction by L17 was only observed in the presence of glucose demonstrates that glucose serves as a necessary carbon source for nitrate reduction by L17 under anoxic conditions.

Nitrate reduction by L17 in the presence of glucose was repressed by the presence of oxygen but insensitive to ammonium (Fig. S4), suggesting that dissimilatory nitrate reduction may take place in L17 [17]. Using reverse transcription–polymerase chain reaction (RT–PCR), dissimilatory nitrate reductase (*nar*Z) and nitrite reductase (*nir*B) were detected with average copy numbers of 2.03×10^7 and 5.53×10^5 per mL sample, respectively, during the nitrate reduction by L17 with glucose (Fig. 2). The *nar*Z and *nir*B genes catalyze the reduction of nitrate to nitrite and the reduction of nitrite to ammonium, respectively [24]. At the end of the incubation (d 14), the amount of NO_2^- and NH_4^+ accounted for approximately 20% and 50% of the initial nitrate, respectively. All of the above results suggest that L17 can dissimilatorily reduce NO_3^- via NO_2^- to NH_4^+ under anoxic conditions.

During nitrate reduction by L17, the concentration of NO increased over time and stabilized after 8 d of incubation, while that of N_2O stabilized at a much lower concentration (Fig. 3). There was 27.9 μmol of NO and 2.28 μmol of N_2O detected at the end of the incubation. The input nitrate was 700 μmol; thus, the transformation ratio for NO + N_2O was approximately 4%. The production of N_2O during nitrate reduction by *Klebsiella* species has been previously reported [27,44], and only 30% of the nitrate in those experiments was converted to N_2O, with the remainder of the nitrate reduced to ammonium [27]. This suggests that L17 is also capable of reducing nitrate to NO and N_2O via denitrification under anoxic conditions.

3.2. Effect of goethite on microbial nitrate reduction

Compared to the L17 treatment, nitrate was reduced completely after 2 d of incubation by L17 in the presence of α-FeOOH (Fig. 1a), and the NO_3^- reduction rate increased markedly to 2.205 d^{-1} (R^2 = 0.998). The presence of α-FeOOH also accelerated NO_2^- formation by L17 at the beginning of the incubation, and accelerated NO_2^- reduction after nitrate was completely reduced (Fig. 1b). The concentration of NH_4^+ increased over time after 2 d in the treatment of L17 + α-FeOOH and was significantly higher than that of L17 (Fig. 1c). At the end of the incubation, both treatments of L17 and L17 + α-FeOOH had similar concentrations of NO_2^- and NH_4^+, and only 29.4 μmol of NO and 3.91 μmol of N_2O were detected in the treatment of L17 + α-FeOOH, with no significant difference from that of L17 (Fig. 3). The above results indicate that the presence of α-FeOOH can accelerate the microbial reduction of nitrate to NO_2^- and NH_4^+ by L17 under anoxic conditions.

To verify the effect of α-FeOOH on nitrite reduction by L17, additional experiments were conducted using nitrite instead of nitrate. During the 14 d incubation, NO_2^- reduction by L17 was also accelerated in the presence of α-FeOOH (Fig. S5a and b), in which NH_4^+ formation was coincidental (Fig. S5c). These results, which are similar to those from the NO_3^- reduction, confirm that α-FeOOH can accelerate the reduction of nitrate and nitrite by L17.

Because L17 can reduce relatively trivial amounts of Fe(III) to achieve a more favorable electron balance during glucose fermentation under anoxic conditions [14], two biotic L17 + α-FeOOH treatments with and without NO_3^-, and abiotic α-FeOOH control experiments were conducted. The formation of dissolved and adsorbed Fe(II) was monitored during the incubation. All treatments exhibited the parallel trend of dissolved Fe(II) formation, the concentrations of which (<0.04 mM) were lower than those of adsorbed Fe(II) (Fig. 4). The L17 + α-FeOOH treatment displayed significantly higher formation of adsorbed Fe(II) than the others. For the L17 + α-FeOOH + NO_3^- treatment, the adsorbed Fe(II) increased at the beginning of the incubation, but decreased after 7 d. At the end of the incubation, 0.258 mM of adsorbed Fe(II) was detected in the L17 + α-FeOOH treatment, whereas less than 0.180 mM were produced in both the L17 + α-FeOOH + NO_3^- and α-FeOOH treatments.

The lower level of Fe(II) generation in the L17 + α-FeOOH + NO_3^- treatment might be due to the competition between nitrate reduction and Fe(III) reduction because both nitrate and Fe(III) oxides can be reduced by L17, which can transfer excess electrons onto the oxidized nitrogen and iron species during fermentation [14,28]. Inhibition of Fe(III) reduction in the presence of nitrate has been reported in some studies [3,12]. The results of the present study demonstrate that the bacterium produced only approximately 0.3 mM of total Fe(II) after 14 d of incubation in the L17 + α-FeOOH treatment. The fact that the rate and extent of nitrate reduction was significantly higher than that of Fe(III) oxide reduction by L17 suggests that the presence of nitrate may inhibit the reduction of Fe(III) by L17.

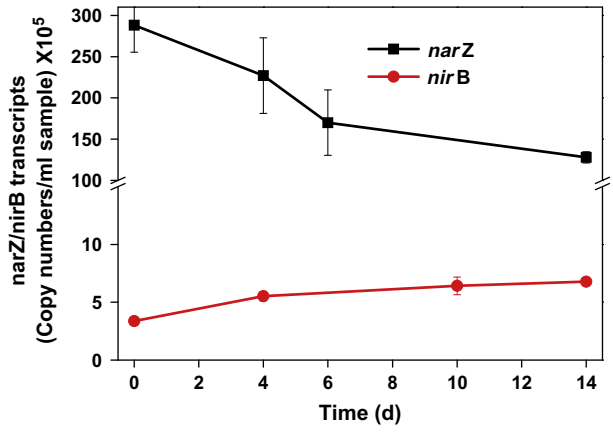

Fig. 2. Expression of *nar*Z and *nir*B, during nitrate reduction in L17 + Glucose + NO_3^- treatment. Initial concentration: 7.5 mM NO_3^-, 10^7 cells mL^{-1} L17, and 5.0 mM glucose in a 30 mM $NaHCO_3$-buffered medium at pH = 6.8. All L17 cultures were grown at 30 °C in anaerobic culture bottles under a 20% CO_2/80% N_2 atmosphere, and all culture manipulations were performed anaerobically. Error bars represent the standard deviation of the mean (n = 3).

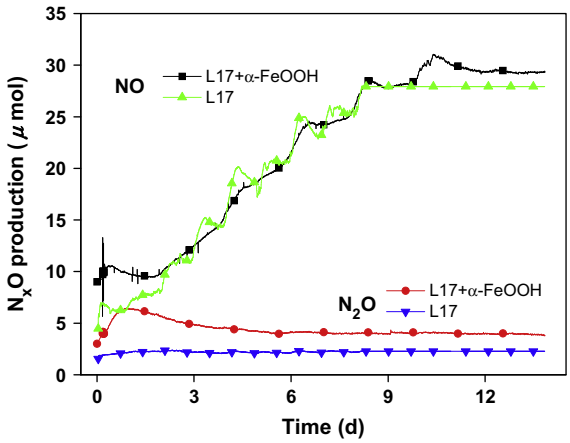

Fig. 3. NO and N_2O formation in the L17 and L17+α-FeOOH treatments. Initial concentration: 7 mM NO_3^-, 4.5 g L^{-1} α-FeOOH, 10^7 cells mL^{-1} L17, and 5.0 mM glucose in a 30 mM $NaHCO_3$-buffered medium at pH = 6.8. No significant concentration of NO or N_2O was detected in the control with medium including glucose and nitrate without addition of cells or iron oxide during the whole reaction time.

Nevertheless, evaluating the role of the Fe(II) species potentially generated by L17 is necessary because the Fe(II) associated with the iron mineral surface is subject to abiotic reduction of NO_3^- under certain conditions [35,36], and biological nitrate-dependent Fe(II) oxidation has been reported in anoxic environments [33,34]. The reoxidation of Fe(II) coupled with nitrate reduction either abiotically or biotically could be an alternative to the inhibition of Fe(III) reduction and enhancement of nitrate reduction.

First, two abiotic treatments of Fe(II) and Fe(II) + α-FeOOH were tested for nitrate reduction, in which neither significant NO_3^-/NO_2^- reduction nor NH_4^+ formation was observed (Figs. 1 and S5). Chemical speciation of aqueous Fe(II) and the surface complex were calculated using Visual MINTEQ 3.0, which revealed that the main species in 0.3 mM Fe(II) without an Fe(III) oxide surface (>FeOH) were Fe^{2+} and $FeHCO_3^+$ and that no siderite was formed, while the main species in Fe(II) + >FeOH included Fe^{2+}, $FeHCO_3^+$, >FeO(FeII)$^+$, and >FehO(FeII)$^+$. This indicates that the aqueous Fe(II) and oxide-adsorbed Fe(II) could not abiotically reduce nitrate or nitrite under anoxic conditions at circumneutral pH in this study. Similarly, no nitrate reduction was observed in the pasteurized nitrate-reducing Fe(II)-oxidizing enrichment culture in the presence of solid phase Fe(II)-bearing minerals [34].

Based on the speciation calculation, the addition of an Fe(III) oxide surface into the Fe(II) treatment can stimulate the adsorption of approximately 23% of Fe(II) onto the surface. According to our previous study [45], no siderite was detected by XRD measurement in the reduction of α-FeOOH by L17. The majority of adsorbed Fe(II) in the L17 + α-FeOOH treatment is bound to the surfaces of L17 cells. Herein, a biotic treatment of L17 + Fe(II) was also conducted, in which the nitrate and nitrite reduction rates were slightly higher than those in L17 treatment (Figs. 1a and S5b). L17 is indicated to be capable of nitrate reduction in the presence of Fe(II), which is similar to a previous report that also used a *Klebsiella* species [32]. Evidence of the reaction between nitrate/nitrite and cell surface-bound ferrous has been demonstrated in microbial Fe(II) oxidation coupled to NO_3^-/NO_2^- reduction [31,42,46], which can be described as the following processes (Eqs. (1)–(4)).

$$4Fe^{2+} + 2NO_3^- + 6H^+ \rightarrow 4Fe^{3+} + NO_2^- + 3H_2O \quad (1)$$

$$Fe^{2+} + NO_2^- + 2H^+ \rightarrow Fe^{3+} + NO + H_2O \quad (2)$$

$$2Fe^{2+} + NO_2^- + 3H^+ \rightarrow 2Fe^{3+} + \frac{1}{2}N_2O + \frac{3}{2}H_2O \quad (3)$$

$$6Fe^{2+} + NO_2^- + 8H^+ \rightarrow 6Fe^{3+} + NH_4^+ + 2H_2O \quad (4)$$

However, the nitrate and nitrite reduction rates of the L17 + Fe(II) treatment were still lower than those of L17 + α-FeOOH treatment (Figs. 1a and S5b), which suggested that the acceleration effect of α-FeOOH on nitrate and nitrite reduction by L17 is not only due to the cell surface-bound Fe(II).

3.3. Effect of other oxides on microbial nitrate reduction

To confirm the acceleration effect of α-FeOOH, the same quantities of other Fe(III) oxides (i.e., γ-FeOOH, α-Fe_2O_3, and γ-Fe_2O_3) were added into the suspension with NO_3^- and L17. As presented in Fig. 5, all Fe(III) oxides accelerated the reduction of NO_3^- by L17, and the nitrate reduction rates normalized to the surface areas of different minerals in the figure inset follow the order of: γ-Fe_2O_3 > α-Fe_2O_3 > γ-FeOOH > α-FeOOH.

Because the growth rates of many organisms (e.g., Fe(III)-reducing bacteria) are coupled with Fe(III) reduction [3,47], the addition of Fe(III) oxides may increase cell numbers, resulting in more nitrate reduction. However, L17 cannot gain any energy for its growth when Fe(III) oxide serves as an electron sink during glucose fermentation [14]. No noticeable increases in cell numbers were observed in any treatments with Fe(III) oxides in the present study. Another possibility is that any Fe(II) produced by L17 can be rapidly microbially reoxidized to Fe(III), with nitrate serving as the electron acceptor [48,49], even though the Fe(III) reduction rate of L17 is lower than the nitrate reduction rate, as discussed earlier. To avoid the potential effect of biogenic Fe(II) generated by L17, TiO_2 and Al_2O_3, non-Fe(III) oxides were added in equivalent quantities to the cell suspension in place of Fe(III) oxides. The results in Fig. 5 demonstrate that both TiO_2 and Al_2O_3 accelerated nitrate reduction by L17, and the normalized nitrate reduction rate with TiO_2 was even higher than the rates with α-FeOOH and γ-FeOOH, whereas that with Al_2O_3 was the lowest. The results with non-Fe(III) oxides suggest that the acceleration of nitrate reduction cannot simply be attributed to biogenic cell surface-bound Fe(II).

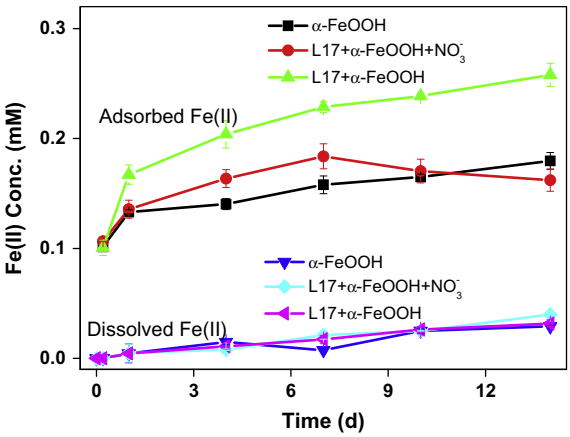

Fig. 4. Adsorbed Fe(II) and dissolved Fe(II) formation in various treatments. Initial concentrations: 7.5 mM NO_3^-, 4.5 g L^{-1} α-FeOOH, 10^7 L17 cells mL^{-1}, and 5.0 mM glucose in a 30 mM $NaHCO_3$-buffered medium at pH = 6.8. Glucose was added in all biotic treatments with L17. Error bars represent the standard deviation of the mean (n = 3).

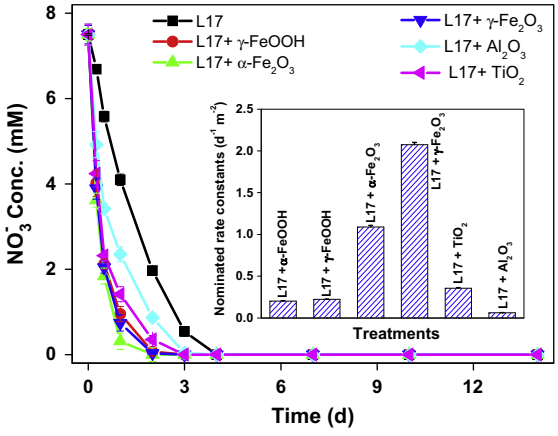

Fig. 5. Microbial NO_3^- reduction by L17 in the presence of various Fe(III) and non-Fe(III) oxides with the normalized rate constants (NRC) to the oxide surface areas displayed in the figure inset. Initial concentrations: 7.5 mM NO_3^-, 10^7 L17 cells mL^{-1}, 5.0 mM glucose, and 4.5 g L^{-1} oxides (i.e., α-FeOOH, γ-FeOOH, α-Fe_2O_3, γ-Fe_2O_3, TiO_2 and Al_2O_3) in a 30 mM $NaHCO_3$-buffered medium at pH = 6.8. Error bars represent the standard deviation of the mean (n = 3). The equation used for calculation of NRCs is: NRC = $k_{L17+oxides}/(S_{oxides} \times M_{oxides})$, wherein S_{oxides} and M_{oxides} represent the specific surface areas and weights of oxides, respectively, and $k_{L17+oxides}$ represents the rate constants of nitrate reduction by L17 in the presence of oxides.

3.4. Effects of Fe(III) and non-Fe(III) oxides on microbial electricity generation

In this study, L17 was demonstrated to be capable of dissimilatory nitrate reduction. However, it is difficult to verify whether Fe(III) oxides can influence the extracellular nitrate reduction by L17 because nitrate is a soluble electron acceptor and can easily enter the cell. L17 has been previously demonstrated to be capable of using an anode as an extracellular electron acceptor in MFCs under anoxic conditions [15], which is an important solid substrate in investigating extracellular electron transfer in microorganisms [37]. In the current study, we used a BEC reactor to study the electricity generation by L17 in the presence of Fe(III) oxides.

Electricity generation in the reactor inoculated with L17 increased to a stable output approximately 45 μA after 4 d, whereas that with L17 + α-FeOOH rose to the highest value at 48 μA after 3 d (Fig. 6a). For the reactors containing L17 in the presence of γ-FeOOH, α-Fe_2O_3, and γ-Fe_2O_3, the highest observed current outputs were 50 μA, 66 μA, and 60 μA, respectively, after 2 d. To clearly evaluate the acceleration effect of Fe(III) oxides on microbial electricity generation, the time dependences of the total coulomb outputs during the incubation were calculated. The results in Fig. 6b verify that all reactors containing L17 + Fe(III) oxides had higher coulomb outputs than those with L17 alone. The ratios of the total coulomb outputs of L17 + Fe(III) oxides to that of L17 are displayed in Fig. 6c. Within 1 d of incubation, the peaks of the ratios were 3.88, 3.15, 2.34, and 1.97 for L17 with α-Fe_2O_3, γ-Fe_2O_3, γ-FeOOH, and α-FeOOH, respectively. These results demonstrate that the addition of Fe(III) oxides could increase the current and coulomb outputs by L17.

To illustrate the potential effect of Fe(II) generated by L17, three experiments with Fe(II), Fe(II) + α-FeOOH, and L17 + Fe(II) were conducted. The results (Fig. 6a) demonstrate that the current output was less than 1 μA throughout the incubation with Fe(II). For Fe(II) + α-FeOOH, the current output increased dramatically at the beginning, mainly due to the oxidation of Fe(II) on the α-FeOOH surface and then decreased sharply as Fe(II) was consumed. The reactor with L17 + Fe(II) maintained a higher rate of current generation (Fig. 6a) and total coulomb output (Fig. 6b) than that of L17, as confirmed by the coulomb output ratio of L17 + Fe(II) to L17 in Fig. 6c. Fe(II) also appeared to accelerate the generation of electricity and coulomb output by L17, although the extent of acceleration was lower than those obtained in the L17 + Fe(III) oxide treatments. Moreover, TiO_2 and Al_2O_3 were used in place of Fe(III) oxides and were added to the L17 suspension in the BEC reactor to avoid the effect of Fe(II). Similarly, the current and coulomb outputs by L17 were enhanced by the presence of these non-Fe(III) oxides (Fig. 6).

Electricity generation is a consequence of the microbial activity of L17, and the establishment of an L17 biofilm on the anode is a key factor for extracellular electron transfer from L17 to the anode in the MFC [15]. In this study, a thick layer composed of cells and Fe(III) oxides was observed after adding Fe(III) oxides into the L17 suspension. The deposit containing cells and Fe(III) oxides was examined using confocal laser scanning microscopy after 1 d of incubation. Fig. 7 demonstrates[2] that many green points (live cells) surround the dark region (Fe(III) oxides) in a red circle, which indicates cell-mineral sorption.

However, the precipitation of Fe(III) oxides and cell-mineral sorption may decrease surface sites on the surface of the anode for direct cell attachment. This would reduce direct electron transfer from cells to the electrode, thereby decreasing electricity generation. Because Fe(III) reduction and electricity generation may occur simultaneously, their contributions must be clearly illustrated. First, the anode can accept an electron from L17 directly (Eq. (5)):

$$\text{Anode} + e^- \xrightarrow{\text{L17}} \text{Anode}^- \quad (5)$$

In the presence of α-FeOOH, reaction of the anode with Fe(II) (Eq. (7)) can follow the reduction of α-FeOOH by L17 (Eq. (6)) [42]:

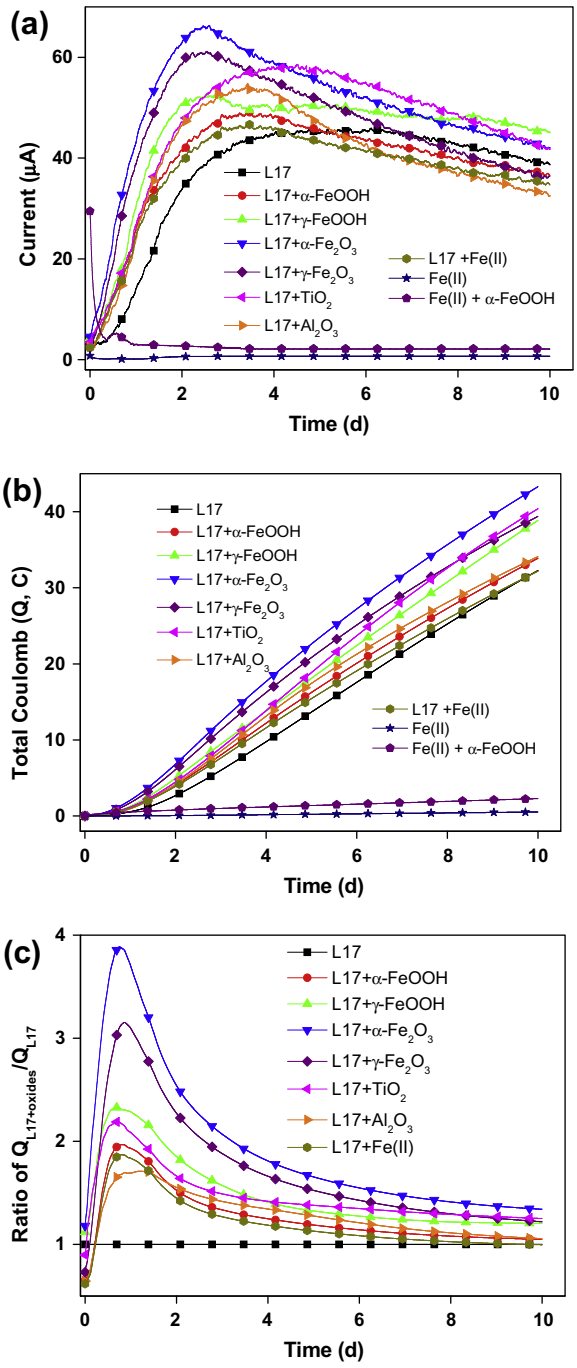

Fig. 6. (a) Electricity generation (μA) in various treatments in the microbial electrochemical cell, (b) total coulomb output (C) with time dependence in various treatments calculated from the data in Fig. 4a, and (c) the calculated ratios of total coulomb outputs of L17 + oxides/Fe(II) to that of L17 alone. Initial concentrations: 7.5 mM NO_3^-, 0.3 mM Fe(II), 10^7 L17 cells mL^{-1}, 5.0 mM glucose, and 4.5 g L^{-1} oxides (i.e., α-FeOOH, γ-FeOOH, α-Fe_2O_3, γ-Fe_2O_3, TiO_2 and Al_2O_3) in a 30 mM $NaHCO_3$-buffered medium at pH = 6.8. Glucose was added in all biotic treatments with L17.

[2] For interpretation of color in Fig. 7, the reader is referred to the web version of this article.

$$\alpha\text{-FeOOH} + e^- \xrightarrow{L17} Fe(II) \quad (6)$$

$$Anode + Fe(II) \rightarrow Anode^- + Fe(III) \quad (7)$$

The surface reduction potential of the anode depends on the cathode electrolyte (ferric cyanide, $E^{o\prime}$ = +0.436 V, pH 7), while the redox potential is +0.770 V for free Fe(II) ions [50], but +0.229 V for Fe(II) on the α-FeOOH surface [51]. Thus, electricity generation is only thermodynamically feasible for the latter reaction. This is verified by the electricity generation results in the treatments of Fe(II) and Fe(II) + α-FeOOH (Fig. 6a). However, the rate of reaction (ii) for Fe(III) reduction (Fig. 4) was evidently lower than that of reaction (i) for electricity generation (Fig. 6), potentially leading to an inhibition of microbial electricity generation. This is contradicted by the observed enhancement of electricity generation in the presence of Fe(III) oxides. Although electricity generation occurred in the Fe(II) + α-FeOOH and L17 + Fe(II) treatments, the generation of Fe(II) was limited by the low rate of microbial α-FeOOH reduction (reaction ii). Obviously, the fact that Fe(III) oxides accelerated the electricity generation by L17 was not completely due to the effect of biogenic Fe(II).

3.5. Possible mechanisms for the acceleration effect of Fe(III) oxides

The present study has clearly demonstrated that nitrate reduction and electricity generation were directly attributed to the microbial activity of L17, both of which could be accelerated in the presence of Fe(III) oxides. Based on the aforementioned results, L17 can drive nitrate reduction and electricity generation in the presence of Fe(II) (possibly cell surface-bound Fe(II)), which can be generated from microbial Fe(III) oxide reduction by L17.

With respect to the effect of cell-mineral sorption, the experimental results using Al_2O_3 as a non-conductive oxide in Figs. 5 and 6 demonstrated that microbial nitrate reduction and electricity generation by L17 could also be enhanced in the presence of Al_2O_3, but with lower effectiveness than for Fe(III) and Ti oxides. This indicates that the cell-mineral sorption does not account for the enhancement of nitrate reduction and electricity generation. However, we found that the acceleration caused by Fe(III) oxides cannot solely be attributed to biogenic Fe(II) and cell-mineral sorption.

Nakamura et al. [39] reported that the addition of α-Fe_2O_3 colloids increased the current generation of *Shewanella loihica* and proposed a semiconductor-mediated electron-hopping process through the interconnected bacterial network, with such nanocolloids promoting a long-distance extracellular electron transfer process to the electrode surface. Hypothetically, the electron transfer rates for nitrate reduction and electricity generation may be accelerated through possible electron transport between cells and Fe(III) oxides because cell-mineral sorption was observed.

When Fe(III) oxide, a known semiconductor, comes into contact with cells, an electron transfer process may occur at the outer membrane enzyme (OME)–Fe(III) oxide interface if the conduction band (CB) of Fe(III) oxide is lower than the electrochemical potential of the OME. This well-known phenomenon has been extensively studied in the field of electrochemistry on semiconductors [52,53]. The redox potential of the OME of L17 was not investigated in this study; however, that of other strains has been reported to be lower than −0.2 V [39]. The normal hydrogen electrode (NHE, pH 7) of CB is −0.133 V for Fe_2O_3 and +0.167 V for FeOOH [54]. There is no thermodynamic energy barrier for the electron transfer process between OME and the CB of Fe(III) oxide. Similarly, such an electron transfer process can also take place between the CB of Fe(III) oxide and an electron acceptor (nitrate or electrode). Reportedly, the redox potential of NO_3^-/NO_2^- is +0.43 V at pH 7 [55], and that of the anode in this study is +0.436 V at pH 7, which is similar to the NHE of the graphite anode, which is usually considered to be approximately +0.50 V [8]. As a result, the order of redox potentials has been ranked as OME < CB of Fe(III) oxide < electron acceptor (nitrate or electrode). Such an energy difference could provide a continuous driving force for the transfer of electrons from cells to Fe(III) oxide to nitrate and the electrode.

Electron transfer from cells to attached Fe(III) oxide can be mediated by *c*-type cytochrome (*c*-Cyt) proteins in the outer membrane of iron-reducing bacteria, e.g., *Shewanella* and *Geobacter* sp. [56], in which heme acts as an active center in the electron-transport chain [57]. Clear evidence for CB-mediated electron transfer between heme and semiconducting TiO_2 was observed using spectroelectrochemical analysis [58]. Additionally, the injection of electrons from heme into the CB of semiconductors has been reported to be very fast, which may lead to fast trapping by some terminal electron acceptors, e.g., nitrate, organic halides, and electrodes [59–62]. In this study, diffuse transmittance absorption was employed to measure the cell suspension of L17, and an absorption spectrum of some *c*-Cyt like species was observed at 420 nm (Fig. S6), which was similar to the *c*-Cyt absorption observed at 410–419 nm in a previous study [63]. This *c*-Cyt like species possibly drives an electron transfer from the OME of L17, to the CB of Fe(III) oxides, to nitrate and the anode, resulting in acceleration of microbial nitrate reduction and electricity generation. The OME-mediated extracellular electron reaction processes from cells to the CB of Fe(III) oxides are presented in following reactions (Eqs. (8) and (9)).

$$CB + e^- \xrightarrow{L17} CB^* \quad (8)$$

$$CB + c - Cyt_{red} \rightarrow CB^* + c\text{-}Cyt_{ox} \quad (9)$$

Subsequently, electrons in the conduction band can be transferred to nitrate or its products via the following reactions (Eqs. (10)–(13)):

$$CB^* + \frac{1}{2}NO_3^- + H^+ \rightarrow CB + \frac{1}{2}NO_2^- + \frac{1}{2}H_2O \quad (10)$$

$$CB^* + NO_2^- + 2H^+ \rightarrow CB + NO + H_2O \quad (11)$$

$$CB^* + \frac{1}{2}NO_2^- + \frac{3}{2}H^+ \rightarrow CB + \frac{1}{4}N_2O + \frac{3}{4}H_2O \quad (12)$$

$$CB^* + \frac{1}{6}NO_2^- + \frac{4}{3}H^+ \rightarrow CB + \frac{1}{6}NH_4^+ + \frac{1}{3}H_2O \quad (13)$$

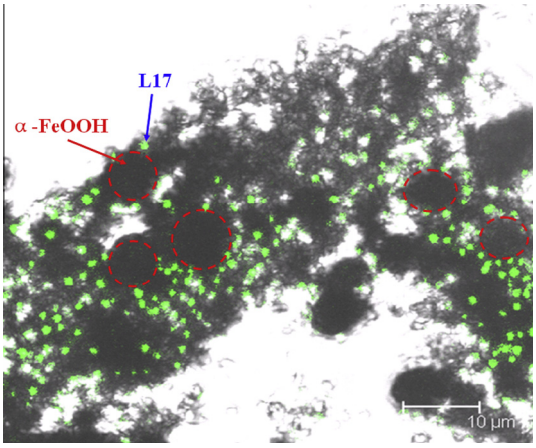

Fig. 7. Confocal laser scanning microscope (CLSM) image of optical cross-section of the L17 + α-FeOOH suspension after 1-d incubation. Initial concentration: 4.5 g L^{-1} α-FeOOH, 10^7 cells mL^{-1} L17, and 5.0 mM glucose in a 30 mM $NaHCO_3$-buffered medium at pH = 6.8.

Electrons in the conduction band can also be directly transferred to the electrode, resulting in current generation (Eq. (14)):

$$CB^{*} + Anode \rightarrow CB + Anode^{-} \quad (14)$$

Semiconductor-mediated electron transfer after cell-mineral adsorption is also considered to contribute to the higher maximum current output and delay of reaching the maximum current output with L17 + TiO_2 when compared to those with L17 + Fe(II), as it is easier and quicker for Fe^{2+} to attach to the cell surface than TiO_2. However, the semiconductor-mediated process needs to be confirmed in further work with clarification regarding whether a *c*-Cyt-like protein is present in the outer membrane of L17 and responsible for the extracellular electron transport of L17 for nitrate reduction and electricity generation. Although electron transfer reactions between bacterial cells, Fe(III) oxides, and electron acceptors are very complicated, the mechanism of semiconductor-mediated electron transfer may provide a direction in the search for possible reactions that occurred in our experiments.

4. Conclusions

The fermentative iron-reducing bacterium *K. pneumoniae* L17 is able to reduce NO_3^- to NO_2^- and NH_4^+ via a dissimilatory nitrate reduction pathway and to NO and N_2O via denitrification under anoxic conditions. The presence of Fe(III) oxides significantly accelerated nitrate reduction and electricity generation by L17, which is only partially attributed to cell surface-bound Fe(II) generated by L17 and cell-mineral sorption. Such a finding is different from the inhibition effect of Fe(III) oxides on nitrate reduction by DIRB, but similar to that observed in another fermentative bacterium, *Bacillus*, which extends the range of bacteria whose nitrate reduction and current generation can be facilitated in the presence of iron oxides. The conduction band of iron oxide is proposed to mediate electron transfer from L17 to nitrate or the electrode, contributing to the acceleration of microbial nitrate reduction and electricity generation. The results obtained in this study not only extend the understanding of nitrate reduction in the natural environment by fermentative bacteria and Fe(III)-bearing minerals but are also helpful for designing and fabricating new bio-electrode materials for studies and applications of MFCs using fermentative bacteria as electrogenic microorganisms and iron oxide as an electrode material.

Acknowledgments

The authors thank the National Natural Science Foundation of China (Nos. 41025003, 41330857, 41340018, and 40901114) and the Natural Science Foundation of Guangdong Province, China (S2011030002882) for financial support for this work.

Appendix A. Supplementary material

Supplementary material associated with this article can be found, in the online version, at http://dx.doi.org/10.1016/j.jcis.2014.02.026.

References

[1] J.A. Gralnick, D.K. Newman, Mol. Microbiol. 65 (2007) 1.
[2] J.K. Fredrickson, J.M. Zachara, Geobiology 6 (2008) 245.
[3] D.R. Lovley, D.E. Holmes, K.P. Nevin, Adv. Microb. Physiol. 49 (2004) 219.
[4] T. Borch, R. Kretzschmar, A. Kappler, P.V. Cappellen, M. Ginder-Vogel, A. Voegelin, K. Campbell, Environ. Sci. Technol. 44 (2010) 15.
[5] F.B. Li, X.M. Li, S.G. Zhou, L. Zhuang, F. Cao, D.Y. Huang, W. Xu, T.X. Liu, C.H. Feng, Environ. Pollut. 158 (2010) 1733.
[6] J. Miot, K. MacLellan, K. Benzerara, N. Boisset, Geobiology 9 (2011) 459.
[7] H.S. Park, B.H. Kim, H.S. Kim, H.J. Kim, G.T. Kim, M. Kim, I.S. Chang, Y.K. Park, H.I. Chang, Anaerobe 7 (2001) 297.
[8] D.E. Holmes, D.R. Bond, D.R. Lovley, Appl. Environ. Microbiol. 70 (2004) 1234.
[9] B.E. Logan, J.M. Regan, Environ. Sci. Technol. 40 (2006) 5172.
[10] B.M. Tebo, A.Y. Obraztsova, FEMS Microbiol. Ecol. 162 (1998) 193.
[11] T. Behrends, P.V. Cappellen, Chem. Geol. 220 (2005) 315.
[12] K.A. Weber, M.M. Urrutia, P.F. Churchill, R.K. Kukkadapu, E.E. Roden, Environ. Microbiol. 8 (2006) 100.
[13] D.C. Cooper, F.W. Picardal, A. Schimmelmann, A.J. Coby, Appl. Environ. Microbiol. 69 (2003) 3517.
[14] X.M. Li, S.G. Zhou, F.B. Li, C.Y. Wu, L. Zhuang, W. Xu, L. Liu, J. Appl. Microbiol. 106 (2009) 130.
[15] X.M. Li, L. Liu, T.X. Liu, T. Yuan, W. Zhang, F.B. Li, S.G. Zhou, Y.T. Li, Chemosphere 92 (2013) 218.
[16] X.M. Li, T.X. Liu, F.B. Li, W. Zhang, S.G. Zhou, Y.T. Li, J. Soils Sediments 12 (2014) 217.
[17] M. Reiche, G. Torburg, K. Kusel, FEMS Microbiol. Ecol. 65 (2008) 88.
[18] F. Picardal, Front. Microbiol. 3 (2012) 112.
[19] W. Zhang, X.M. Li, T.X. Liu, F.B. Li, W.J. Shen, Colloid Surf. A 445 (2014) 97.
[20] S. Schädler, C. Burkhardt, F. Hegler, K.L. Straub, J. Miot, K. Benzerara, A. Kappler, Geomicrobiol. J. 26 (2009) 93.
[21] S.H. Kopf, C. Henny, D.K. Newman, Environ. Sci. Technol. 47 (2013) 2602.
[22] E.E. Roden, Biochem. Soc. Trans. 40 (2012) 1249.
[23] A.J. Coby, F. Picardal, E. Shelobolina, H. Xu, E.E. Roden, Appl. Environ. Microbiol. 77 (2011) 6036.
[24] C. Moreno-Vivián, P. Cabello, M. Martínez-Luque, R. Blasco, F. Castillo, J. Bacteriol. 181 (1999) 6573.
[25] P. Cabello, M.D. Roldan, C. Moreno-Vivian, Microbiology 150 (2004) 3527.
[26] P.J. Gonzalez, C. Correia, I. Moura, C.D. Brondino, J.J.G. Moura, J. Inorg. Biochem. 100 (2006) 1015.
[27] B.H. Bleakley, J.M. Tiedje, Appl. Environ. Microbiol. 44 (1982) 1342.
[28] J.M. Tiedje, in: A.J.B. Zehnder (Ed.), Biology of Anaerobic Microorganisms, John Wiley, New York, 1988, p. 179.
[29] V. Stewart, Antonie van Leeuwenhoek 66 (1994) 37.
[30] G. Pinar, J.L. Ramos, Appl. Environ. Microbiol. 64 (1998) 5016.
[31] A. Kappler, B. Schink, D.K. Newman, Geobiology 3 (2005) 235.
[32] J.M. Senko, T.A. Dewers, L.R. Krumholz, Appl. Environ. Microbiol. 71 (2005) 7172.
[33] K.L. Straub, M. Benz, B. Schink, F. Widdel, Appl. Environ. Microbiol. 62 (1996) 1458.
[34] K.A. Weber, F.W. Picardal, E.E. Roden, Environ. Sci. Technol. 35 (2001) 1644.
[35] H.C.B. Hansen, C.B. Koch, H. Nancke-Krogh, O.K. Borggaard, J. Sørensen, Environ. Sci. Technol. 30 (1996) 2053.
[36] C.J. Ottley, W. Davison, W.M. Edmunds, Geochim. Cosmochim. Acta 61 (1997) 1819.
[37] K. Rabaey, W. Verstraete, Trends Biotechnol. 23 (2005) 291.
[38] A. Thygesen, F.W. Poulsen, B. Min, I. Angelidaki, A.B. Thomsen, Bioresour. Technol. 100 (2009) 1186.
[39] R. Nakamura, F. Kai, A. Okamoto, G.J. Newton, K. Hashimoto, Angew. Chem. Int. Ed. 44 (2009) 508.
[40] W. Zhang, X.M. Li, T.X. Liu, F.B. Li, J. Soils Sediments 12 (2012) 354.
[41] X.G. Wang, C.S. Liu, X.M. Li, F.B. Li, S.G. Zhou, J. Hazard. Mater. 153 (2008) 426.
[42] J. Miot, K. Benzerara, G. Morin, S. Bernard, O. Beyssac, E. Larquet, A. Kappler, F. Guyot, Geobiology 7 (2009) 373.
[43] T. Paul, P.L. Miller, T.J. Strathmann, Environ. Sci. Technol. 41 (2007) 4720.
[44] T. Satoh, S.S.M. Hom, K.T. Shanmugam, J. Bacteriol. 155 (1983) 454.
[45] T.X. Liu, X.M. Li, F.B. Li, W. Zhang, M.J. Chen, S.G. Zhou, Colloids Surf., A 379 (2011) 143.
[46] A.J. Coby, F.W. Picardal, Appl. Environ. Microbiol. 71 (2005) 5267.
[47] S. Kim, F.W. Picardal, Environ. Toxicol. Chem. 18 (1999) 2142.
[48] K.T. Finneran, M.R. Housewright, D.R. Lovley, Environ. Microbiol. 4 (2002) 510.
[49] C.J. Jørgensen, O.S. Jacobsen, B. Elberling, J. Aamand, Environ. Sci. Technol. 43 (2009) 4851.
[50] B. Thamdrup, in: Bernhard Schink (Ed.), Advances in Microbial Ecology, Kluwer Academic/Plenum Publishers, New York, 2000, p. 41.
[51] L. Tao, F.B. Li, Y.K. Wang, K.W. Sun, Clays Clay Miner. 58 (2010) 682.
[52] Y. Xu, M.A.A. Schoonen, Am. Miner. 85 (2000) 543.
[53] L. Yang, C.I. Steefel, M.A. Marcus, J.R. Bargar, Environ. Sci. Technol. 44 (2010) 5469.
[54] E.A. Davidson, J. Chorover, D.B. Dail, Global Change Biol. 9 (2003) 228.
[55] H.R. Beller, Appl. Environ. Microbiol. 71 (2005) 2170.
[56] M.E. Hernandez, D.K. Newman, Cell. Mol. Life Sci. 58 (2001) 1562.
[57] S. Mori, K. Ishii, Y. Hirakawa, R. Nakamura, K. Hashimoto, Inorg. Chem. 50 (2011) 2037.
[58] A. Staniszewski, A.J. Morris, T. Ito, G.J. Meyer, J. Phys. Chem. B 111 (2007) 6822.
[59] M.R. Hoffmann, S.T. Martin, W. Choi, B.W. Bahnemann, Chem. Rev. 95 (1995) 69.
[60] D. Mimica, J.H. Zagal, F. Bedioui, J. Electroanal. Chem. 497 (2001) 106.
[61] S.O. Obare, T. Ito, M.H. Balfour, G.J. Meyer, Nano Lett. 3 (2003) 1151.
[62] J.R. Stromberg, J.D. Wnuk, R.A.F. Pinlac, G.J. Meyer, Nano Lett. 6 (2006) 1284.
[63] R. Nakamura, K. Ishii, K. Hashimoto, Angew. Chem. Int. Ed. 48 (2009) 1606.